IEEE Photonics Journal
An IEEE Photonics Society Publication

Open Access

Polarization Multiplexed Optical OFDM System With a Beat Interference Cancellation Receiver

Volume 12, Number 6, December 2020

Jianxin Ma, *Member, IEEE*
Zhiqi Hu

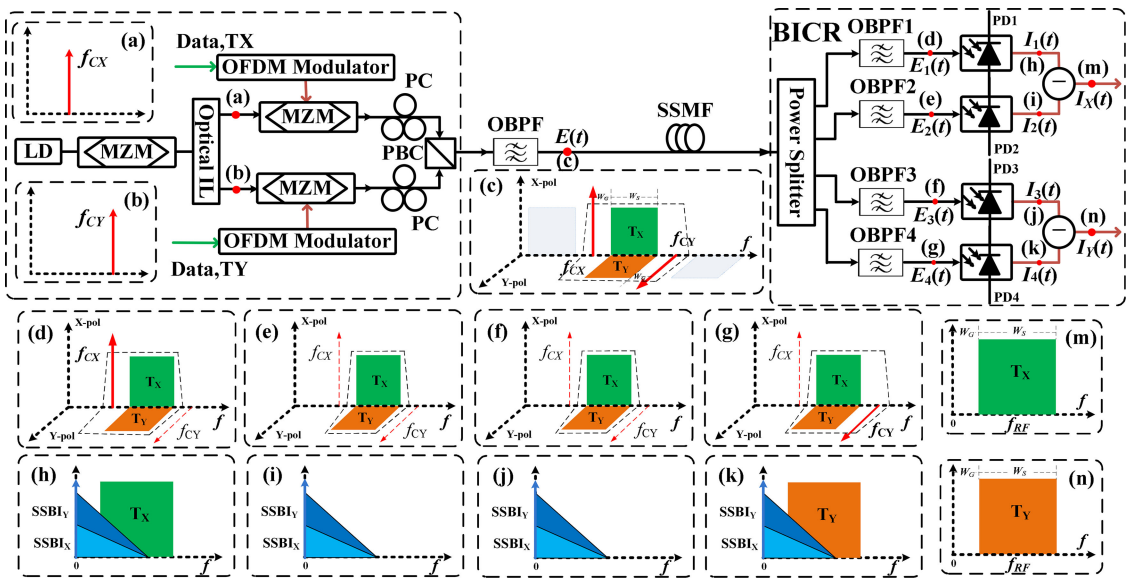

DOI: 10.1109/JPHOT.2020.3036030

Polarization Multiplexed Optical OFDM System With a Beat Interference Cancellation Receiver

Jianxin Ma, *Member, IEEE*, and Zhiqi Hu

State Key Laboratory of Information Photonics and Optical Communications and Beijing Key Laboratory of Space-Ground Interconnection and Convergence, School of Electronic Engineering, Beijing University of Posts and Telecommunications, Beijing 100876, China

DOI:10.1109/JPHOT.2020.3036030

Manuscript received August 6, 2020; revised October 23, 2020; accepted October 27, 2020. Date of publication November 9, 2020; date of current version December 4, 2020. This work was supported in part by the National Natural Science Foundation of China (NSFC) under Grant 61690195 and in part by the Funds of State Key Laboratory of IPOC (IPOC2018ZT09, IPOC2020ZT06). Corresponding author: Jianxin Ma (e-mail: majianxinxy@163.com).

Abstract: A novel beat interference cancellation receiver (BICR) is proposed to cancel the signal-signal beat interference (SSBI) for polarization division multiplexed (PDM) optical orthogonal frequency division multiplexing (OOFDM) system, where two single sideband (SSB) OOFDM signals are polarization multiplexed along with their offset optical carriers (OCs) located at opposite sides. At receiver, the PDM SSB-OOFDM signal is equally power split into four beams with one or two OCs filtered out, and then fed into two balanced photodiode pairs for recovering the RF-OFDM signals with SSBI cancellation. The PDM SSB-OOFDM system is insensitive to fiber polarization mode dispersion since the proposed BICR is implemented without polarization-sensitive devices. Moreover, the spectral efficiency is greatly improved because of PDM and the small guard band since the SSBIs are eliminated. The proposed BICR scheme is validated with a simulation link of 112 Gbps 16-QAM PDM SSB-OOFDM signals. After 120km SSMF transmission, the EVM keeps below forward error correction limit of 16.3%.

Index Terms: Optical orthogonal frequency-division multiplexing (O-OFDM), Polarization division multiplexing (PDM), signal-signal beat interference (SSBI) cancellation.

1. Introduction

With the advent of 5G and big data, more and more terminal devices are connected to the network, which leads to exploding increase of the transmission capacity requirements. The optical communication systems with high capacity and spectrum efficiency (SE) become a research hotspot for short- and medium-distance scenarios [1]–[5]. Orthogonal frequency division multiplexing (OFDM) technology is being considered in research for future optical communication due to its potentially higher SE and compatible with the DSP [6]–[10]. Coherent optical (CO) OFDM system has merits of higher SE, higher receiving sensitivity and better robustness to both fiber chromatic dispersion (CD) and polarization mode dispersion (PMD), but both its transmitter and receiver require narrow-linewidth lasers [11]. In addition, the DSP and MIMO technologies are required to deal with the frequency and phase offsets as well as the polarization rotation of the optical OFDM signal. In contrast, intensity modulation with direct detection (IM/DD) optical OFDM system is insensitive to frequency and phase offsets since both the OOFDM signal and its optical carrier (OC) come

from the same laser diode (LD) and have synchronous frequency and phase fluctuations even after synchronously transmitted over the fiber. Compared with intensity modulation direct detection system with double sideband (DSB) optical spectrum, the single sideband (SSB) OOFDM system can avoid the power fading and bit walk effects caused by the CD, but, in the photocurrent, the signal-signal beat interference (SSBI) may overlap with the RF-OFDM signal in frequency domain, which degrades the link performance and limits the SE [12], [13]. Methods have been proposed to eliminate the SSBI for reducing the guard band (GB). In [12]–[17], several beat interference cancellation receivers (BICRs) have been proposed based on balance detection. In addition, iterative estimation and cancellation techniques [18], [19], KK receivers [20]–[22] were proposed for mitigating the SSBI. However, these methods are designed for eliminating the SSBI in a single polarization system but can't be used to the polarization-multiplexed OOFDM system directly.

Polarization division multiplexing (PDM) technology can double the system capacity and SE by transmitting two OFDM signals on two orthogonally polarized modes of the lightwave. However, since the fiber PMD rotates the two orthogonally modes randomly, the OOFDM signals carried by the two modes are coupled with each other and can never be split directly by a polarization beam splitter (PBS) without costly polarization stabilizer. MIMO algorithms with digital signal processing have been proposed to deal with the PMD [23]–[26]. Besides the PMD, in the PDM SSB-OOFDM system, the SSBIs also need to be suppressed to improve the SE. Several beat interference cancellation techniques specifically for PDM SSB-OOFDM systems with reduced GB have been proposed to eliminate SSBIs in [26], [27]. In 2019, we have proposed a misaligned optical carrier (MOC) PDM SSB-OOFDM system based on a single BICR to avoid the PMD [28], but the SE is low since the misaligned OCs at the same sideband leave a blank spectrum gap. Recently, Canadian scholars proposed an asymmetric direct detection (ADD) for canceling the SSBI in the PDM SSB-OOFDM system with orthogonal offset carriers [29]. The photocurrent difference between the X- and Y polarization directions is used to eliminate the interference without an iterative algorithm. ADD not only reduces the complexity of signal linearization, but also simplifies the receiver equipment. However, iterative algorithm and KK method are needed to recover two SSB-OOFDM signals.

In this paper, we report a PDM SSB-OOFDM system with a novel BICR for the PDM SSB-OOFDM signal with the orthogonal OOFDM signals overlapping in frequency domain and their offset OCs located on opposite sides. In the proposed BICR, the PDM SSB-OOFDM signal after fiber transmission is split into four beams with equal power. After suppressing one or two OCs properly by optical bandpass filters (OBPFs), the four optical signals are photodetected by two pairs of the balanced photodetector (BPD) pairs with the undesired SSBIs cancellation. This proposed PMD SSB-OOFDM system can not only eliminate SSBI to reduce the GB, but also resist the PMD without MIMO technology and polarization stabilizer. To demonstrate our proposed PDM SSB-OOFDM system scheme, a simulation link is built with 112 Gbps 16-QAM PDM-SSB-OOFDM signal. The performance of the link is estimated based on error vector magnitude (EVM) and constellations. The simulation results show that the EVMs maintain below the forward error correction (FEC) limit of 16.3% after 120 km standard single-mode fiber (SSMF) transmission.

2. Principle of the MOC PDM-SSB-OOFDM Link

A schematic diagram of the PDM SSB-OOFDM system with our proposed BICR is depicted in Fig. 1. In the transmitter, two baseband OFDM signals, $S_X(t)$ and $S_Y(t)$, are generated by the OFDM modules, and can be expressed in complex as

$$S_k(t) = \sum_{i=0}^{i=\infty} \left[\sum_{n=-\frac{N}{2}}^{n=\frac{N}{2}-1} C_{ni}^{k} \Pi(t - iT) e^{j\omega_n t} \right] \tag{1}$$

where $k = X, Y$; i is the index of the OFDM symbol; N is the number of subcarriers; C_{ni}^{k} is the complex symbols carried by the n^{th} subcarrier of the i^{th} OFDM symbol on k polarization mode; $\Pi(t)$

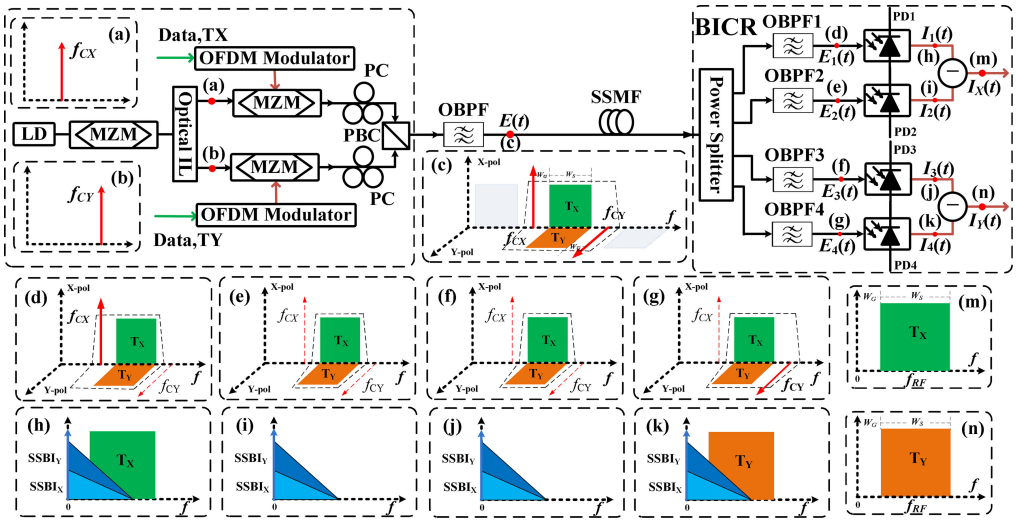

Fig. 1. Schematic of PDM SSB-OOFDM system with proposed BICR. LD, laser diode; MZM: Mach-Zehnder modulator; Optical IL: Optical interleaver; OFDM Modulator: orthogonal frequency division multiplexing modulator; I/Q mod: I/Q modulator; OBPF: optical band-pass filter; PC: Polarization control; PBC: polarization beam combiner; SSMF: standard single mode fiber; PD: photodetector.

is the rectangular pulse shaping function with the value of 1 at $0<t\leq T$ and 0 otherwise; T is the OFDM symbol duration; $\omega_n = 2\pi f_n = 2\pi n/T$ is the angular frequency of the n^{th} subcarrier of the baseband OFDM signal; Since $-N/2\leq n<N/2-1$, the bandwidth of the baseband OFDM signal is $W_S = N/T$. Then, the complex envelopes of two baseband OFDM signals are modulated on the RF carrier at $f_{RF} = \omega_{RF}/2\pi > W_S/2$ by I/Q modulator (I/Q Mod) and produce the two RF OFDM signals $V_{RFX}(t)$ and $V_{RFY}(t)$, which can be expressed as

$$\begin{aligned} V_{RFk}(t) &= V_{RF}\left[\text{Re}\left\{S_k(t)\right\}\cos\left(\omega_{RFk}t\right) - \text{Im}\left\{S_k(t)\right\}\sin\left(\omega_{RFk}t\right)\right] \\ &= V_m a_k(t)\cos\left[\omega_{RFk}t + \varphi_k(t)\right] \end{aligned} \tag{2}$$

where $k = X, Y$; $V_m a_k(t) = |V_{RF}S_k(t)|$ and $\varphi_k(t) = arg(S_k(t))$ represent the amplitude and phase of the RF OFDM signal, respectively; $a_k t)$ represents the normalized amplitude of the RF OFDM signal. Here f_{RFX} and f_{RFY} are equal to f_{RF} and represent the center frequency of RF OFDM signals to be modulated on X- and Y-polarizations, respectively, and so the subcarriers are located in $[f_{RF} - W_S/2,\ f_{RF} + W_S/2]$ with a GB of $W_G = f_{RF} - W_S/2$. The OCs, $E_{inX}(t) = E_C\exp(j2\pi f_{CX}t)$ and $E_{inY}(t) = E_C\exp(j2\pi f_{CY}t)$, are generated by separating two first-order optical sidebands via an optical interleaver (IL), which is generated by OC suppression modulation the lightwave at f_o from the laser diode with the RF local oscillator at the frequency of f_{RF}, as shown in Fig. 1 (a) and (b). The two OCs are modulated by the RF-OFDM signals to generate two DSB OOFDM signals with one OOFDM signal sideband overlapping with the others in frequency domain since they meet the relationship $f_{CX} + f_{RFX} = f_{CY} - f_{RFY} = f_o$. Then they are orthogonally combined by polarization beam combiner (PBC) along with polarization controls (PCs), and an optical bandpass filter (OBPF) with the bandwidth a little larger than $(\mathrm{W_S} + 2\mathrm{W_G})$ is used to filter out the sidebands and noises outside the two OCs to form the PDM SSB-OOFDM signal,

$$\begin{aligned} \vec{E}(t) &\approx \frac{\alpha}{2}E_C\hat{e}_x\left\{\left(1-e^{j\frac{\pi\Delta}{V_\pi}}\right)e^{j2\pi f_{CX}t} + \frac{1}{2}\left(1+e^{j\frac{\pi\Delta}{V_\pi}}\right)jm_{hX}a_X(t)e^{j[2\pi f_o t+\varphi_X(t)]}\right\} \\ &\quad + \frac{\alpha}{2}E_C\hat{e}_y\left\{\left(1-e^{j\frac{\pi\Delta}{V_\pi}}\right)e^{j2\pi f_{CY}t} + \frac{1}{2}\left(1+e^{j\frac{\pi\Delta}{V_\pi}}\right)jm_{hY}a_Y(t)e^{j[2\pi f_o t-\varphi_Y(t)]}\right\} \\ &\doteq \hat{e}_x\left[E_{CX}(t)+E_{SX}(t)\right] + \hat{e}_y\left[E_{CY}(t)+E_{SY}(t)\right] = \hat{e}_x E_X(t) + \hat{e}_y E_Y(t) \end{aligned} \tag{3}$$

where $\hat{e}_x$and $\hat{e}_y$ are mutually orthonormal vectors; Δ denotes the deviated DC bias voltage relative to the minimum transmission point of each MZM and is small relative to its half-wave voltage V_π. For simplifying the deduction below, we assume $E_{Ck}(t) = \frac{\alpha}{2}E_C(1 - e^{j\frac{\pi\Delta}{V_\pi}})e^{j2\pi f_{Ck}t}$, $E_{Sk}(t) = \frac{\alpha}{4}E_C(1 + e^{j\frac{\pi\Delta}{V_\pi}})\,jm_{hk}a_k(t)e^{j[2\pi f_o t+\varphi_k(t)]}$ with $k = X, Y$, and $E_{CX}(t) + E_{SX}(t) = E_X(t)$, $E_{CY}(t) + E_{SY}(t) = E_Y(t)$. By adjusting the bias voltage of Δ, we can vary the carrier-to-signal power ratio (CSPR) of the generated SSB-OOFDM signal. Although the reduction of the CSPR can improve its effective optical signal-to-noise ratio (OSNR), small CSPR will increase the influence of both intra- and inter-polarization SSBI [27], [30]. In view of the trade-off between the OSNR and SSBI, the CSPR was optimized by adjusting Δ. In order to realize a high SE, since the spectral of two OOFDM sideband signals are overlapped with each other, the PDM SSB-OOFDM signal has a high SE. Fig. 1(c) diagrams the optical spectrum of the PDM SSB-OOFDM signal, which, of course, can also be generated in different ways [27].

As the PDM SSB-OOFDM signal is transmitted over the SSMF, although both the OCs and OOFDM sideband signals suffer from random polarization rotation, their rotation is completely synchronous and so their polarization states remain orthogonal instantly in a new Cartesian coordinates. After fiber transmission, the PDM SSB-OOFDM signal is received by our proposed BICR. In BICR, the PMD SSB-OOFDM signal is equally power split into four beams by a polarization-insensitive power splitter. Then, each of them passes through a polarization-insensitive optical bandpass filter (OBPF) or optical notch filter to suppress the undesired OC. For the first beam, the OC of Y-polarization, $E_{CY}(t)$, is filtered out, while the OOFDM signal of Y-polarization and both the OC and OOFDM signal of X-polarization, $E_{CX}(t)$ and $E_{SX}(t)$, are output,

$$\vec{E}_1(t) = \frac{1}{4}\left[\hat{e}_x\left(E_{CX}(t) + E_{SX}(t)\right) + \hat{e}_y E_{SY}(t)\right] \tag{4}$$

For the second beam, two OCs, $E_{CX}(t)$ and $E_{CY}(t)$, are filtered out and only the two orthogonal OOFDM signals are output,

$$\vec{E}_2(t) = \frac{1}{4}\left[\hat{e}_x E_{SX}(t) + \hat{e}_y E_{SY}(t)\right] \tag{5}$$

Their optical spectra are shown in Fig. 1(d) and (e). Then, they are fed to the first BPD and generate the photocurrents,

$$I_1(t) = \mu\left|\vec{E}_1(t)\right|^2 = \frac{\mu}{16}\left\{\left|E_{SX}(t)\right|^2 + \left|E_{SY}(t)\right|^2 + \left[E_{SX}(t)E_{CX}^*(t) + E_{SX}^*(t)E_{CX}(t)\right] + \left|E_{CX}(t)\right|^2\right\} \tag{6}$$

$$I_2(t) = \mu\left|\vec{E}_2(t)\right|^2 = \frac{\mu}{16}\left[\left|E_{SX}(t)\right|^2 + \left|E_{SY}(t)\right|^2\right] \tag{7}$$

where the two PDs in the BPD pair have identical sensitivity of μ. Here $|E_{CX}(t)|^2$ is a DC component generated by the self-beating of the OC, $|E_{SX}(t)|^2$ and $|E_{SY}(t)|^2$ are the SSBIs generated by the self-beating of the two OOFDM signals, and $[E_{CX}(t)E_{SX}*(t) + E_{CX}*(t)E_{SX}(t)] = 2\mathrm{Re}\{E_{CX}*(t)E_{SX}(t)\}$ is the desired RF OFDM signal generated by the heterodyne beating of the OC and OOFDM signal. Their RF spectra are shown in Fig. 1(h) and (i). Since the photocurrent of the first beam consists of the heterodyne beating $\mathrm{Re}\{E_{CX}*(t)E_{SY}(t)\}$ and self-beatings of $|E_{CX}(t)|^2$, $|E_{SX}(t)|^2$ and $|E_{SY}(t)|^2$, while that of the second beam consists only of the two self-beating, $|E_{SX}(t)|^2$ and $|E_{SY}(t)|^2$, the differentiate photocurrent output from the BPD includes only $|E_{CX}(t)|^2$ and $\mathrm{Re}\{E_{CX}*(t)E_{SX}(t)\}$, namely,

$$\begin{aligned} I_X(t) = I_1(t) - I_2(t) = &-\frac{\mu\alpha^2 {E_C}^2 \pi V_m}{32V_\pi}\sin\left(\pi\frac{\Delta}{V_\pi}\right)\mathrm{Re}\left\{a_X(t)e^{j(2\pi f_{RFX}t+\varphi_X(t))}\right\} \\ &+ \frac{\mu\alpha^2 {E_C}^2}{32}\left[1 - \cos\left(\pi\frac{\Delta}{V_\pi}\right)\right] \end{aligned} \tag{8}$$

It can be seen that the SSBIs are cancelled completely and the BPD outputs only the desired RF OFDM signal modulated on the X-polarization, as indicated by $a_X(t)$ and $\varphi_X(t)$, with a DC bias, as shown by the spectrum in Fig. 1(m).

The third beam is processed in the same way as the second beam, while, for the fourth beam, the OC of X-polarization, $E_{CX}(t)$, is filtered out, and the OOFDM signal of X-polarization and both the OC and OOFDM signal of Y-polarization, $E_{CY}(t)$ and $E_{SY}(t)$, are left. So they become

$$\vec{E}_3(t) = \frac{1}{4}\left[\hat{e}_x E_{SX}(t) + \hat{e}_y E_{SY}(t)\right] \tag{9}$$

$$\vec{E}_4(t) = \frac{1}{4}\left[\hat{e}_x E_{SX}(t) + \hat{e}_y \left(E_{CY}(t) + E_{SY}(t)\right)\right] \tag{10}$$

Their diagrammatic optical spectra after optically filtering are shown in Fig. 1 (f) and (g). After photodetection by a second BPD, the output differentiate photocurrent can be expressed as,

$$I_Y(t) = \mu\left|\vec{E}_4(t)\right|^2 - \mu\left|\vec{E}_3(t)\right|^2 = \frac{-\mu\alpha^2 {E_C}^2 \pi V_m}{32 V_\pi} \sin\left(\pi\frac{\Delta}{V_\pi}\right) \mathrm{Re}\left\{a_Y(t) e^{-j(2\pi f_{RFY} t + \varphi_Y(t))}\right\} + \frac{\mu\alpha^2 {E_C}^2}{32}\left[1 - \cos\left(\pi\frac{\Delta}{V_\pi}\right)\right] \tag{11}$$

It can be seen that only the desired RF OFDM signal modulated on the Y-polarization, as indicated by $a_Y(t)$ and $\varphi_Y(t)$, is output from the BPD with a DC bias while the SSBIs are cancelled. The corresponding RF spectra of the photocurrents of third and fourth beams are shown as Fig. 1(j) and (k) and Fig. 1 (n) shows the desired RF OFDM signal spectrum on the Y polarization with the SSBI cancelled. Since the SSBIs are eliminated, the GB between the OC and OOFDM signals is expected to reduce greatly, which means a higher SE. Moreover, the PDM SSB-OOFDM system is insensitive to fiber polarization mode dispersion because the proposed BICR is implemented without polarization-sensitive devices.

3. Simulation Setup and Results

In order to verify our proposed PDM SSB-OOFDM system scheme, a simulation link with 112Gbps 16-QAM PDM SSB-OOFDM signal was built, as shown in Fig. 2.

In order to verify our proposed PDM SSB-OOFDM system scheme, a simulation link with 112 Gbps 16-QAM PDM SSB-OOFDM signal was built, as shown in Fig. 2. At the transmitter, the lightwave from a continuous wave laser diode (CW LD) with 1MHz linewidth is modulated by the RF local oscillator signal via a Mach-Zehnder modulator (MZM1) in OCS pattern with a DC bias voltage of $0.5V_\pi$. The generated $\pm 1^{st}$-order sidebands, as shown in Fig. 2(c), are separated by an optical IL and work as the OCs of the X- and Y-polarizations. To generate the OFDM signal for the X-polarization, a pseudo random bit sequence (PRBS) with the length of 65535 and bit rate of 56 Gbps is mapped into 16384 16-QAM symbols; then, the 16-QAM symbols are serial-to-parallelly converted to facilitate 128-subcarrier modulation by inverse fast Fourier transform (IFFT) and form 128 OFDM symbols; next, a cyclic prefix consisting of 32 sample points is added for each OFDM symbol to resist the inter-symbol interference; at last, the analog baseband OFDM signal is obtained after parallel-to-serial conversion and digital-to-analog conversion. The baseband OFDM signal is upconverted to the RF OFDM signal with 14 GHz bandwidth by mixing with a RF carrier with the tunable frequency from 8 to 25 GHz, which corresponds to a GB varying from 1 to 18 GHz. The other RF OFDM signal for the Y-polarization is generated in the same way but with a second PRBS. Fig. 2 (a) and (b) show their spectra of the RF OFDM signals with the RF carrier frequency of 9 GHz. The two RF OFDM signals are respectively modulated onto the OCs to generate the DSB OOFDM signals by driving MZM2 and MZM3 with the half-wave voltage of $V_\pi = 4$ V and $\Delta = 0.58$ V resulting in $V_{bias} = V_\pi - \Delta = 3.42$ V. The generated two DSB OOFDM signals, as shown in Fig. 2(d) and (e), are polarization multiplexed via a PBC after rotating the polarization states orthogonal, and then are converted to the PDM SSB-OOFDM signal by a Gaussian OBPF

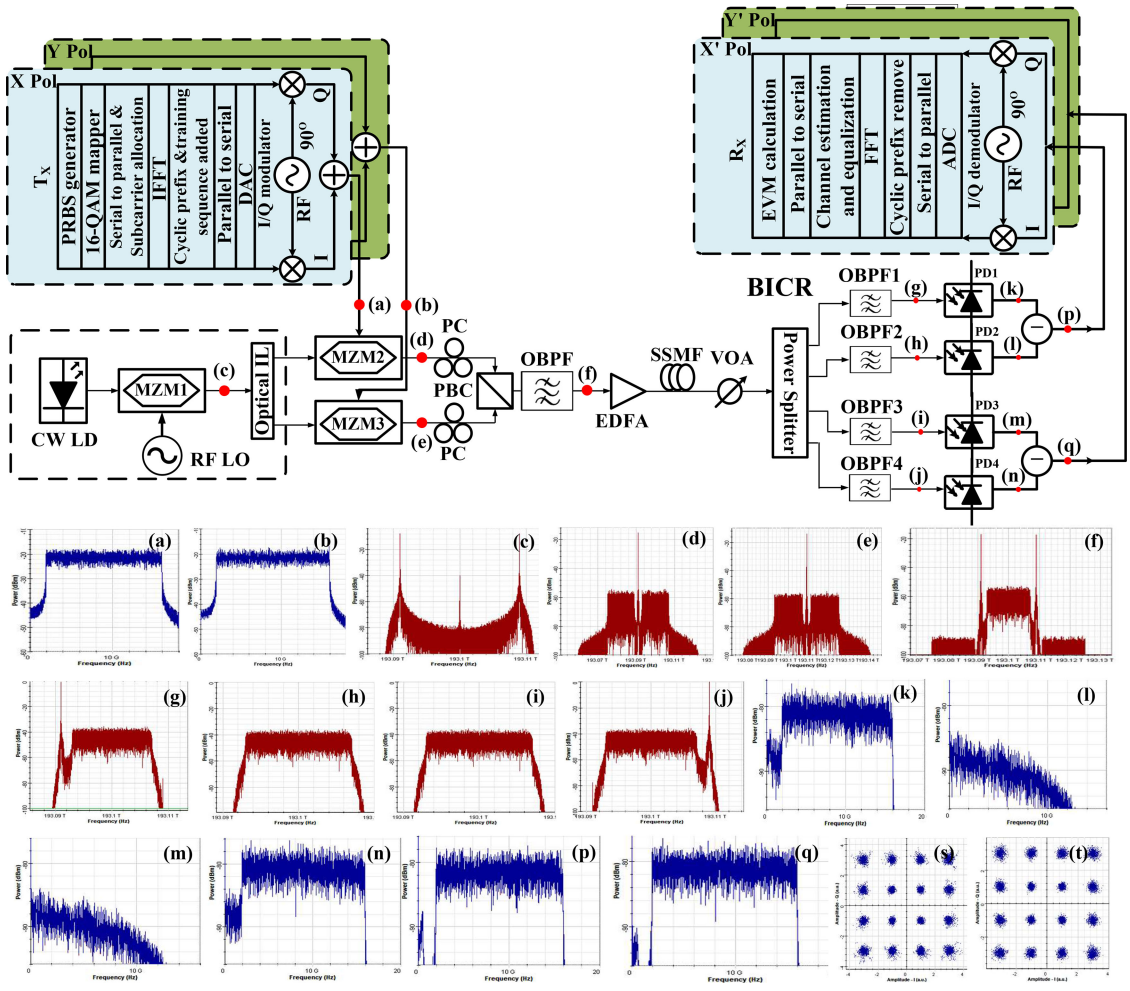

Fig. 2. Simulation link of PDM SSB OOFDM system with BICR we proposed. The 16 illustrations in Fig. 2 represent the spectrum at different locations in the simulation link. The illustrations (a) and (b) represent the spectrum of the RF OFDM signal to be carried in the X and Y polarization directions, respectively; (c) represents two optical carriers used to modulate two RF OFDM signals; (d) and (e) represent the DSB OOFDM signals in the X and Y polarization directions, respectively; (f) represents the PDM SSB OOFDM signal transmitted in the fiber; (g)–(j) represent the PDM SSB OOFDM signals filtered by the optical filter of the four branches respectively; (k)–(n) represent the spectrum of the photocurrent of the four branches after photoelectric conversion; (p) and (q) represent the spectrum of the RF OFDM signal after the SSBI cancellation in the X and Y polarization directions, respectively; (s) and (t) show the constellation after demodulation in X and Y polarization directions, respectively.

with bandwidth of 19 GHz and central frequency of 193.1THz, whose optical spectrum is shown in Fig. 2(f). It can be calculated that the SE of the system is improved to 6.22bit/s/Hz for the GB of 2 GHz. Here, the CSPR of the SSB-OOFDM signal is set to 12dB as $\Delta = 0.58$ V according to the optimization in [27], [30]. Then, the PDM SSB-OOFDM signal is power enhanced to 3dBm by an Erbium-doped fiber amplifier (EDFA) and then launched into the SSMF with the CD coefficient of 16ps/nm·km, PMD coefficient of 0.2 ps/km$^{1/2}$, loss coefficient of 0.2 dB/km. After transmission, the PDM SSB-OOFDM signal is received by the proposed BICR. An EDFA is used for adjusting the optical power injecting into the receiver.

In the BICR, the PDM SSB-OOFDM signal is equally power split into four beams by a power splitter. Then four PDM SSB-OOFDM signals are filtered by different Gaussian OBPFs with steep

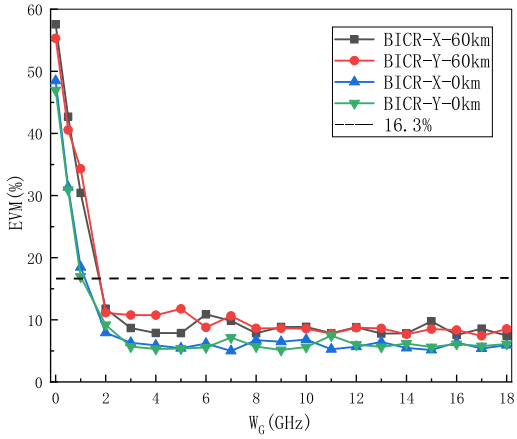

Fig. 3. EVM versus GB at OBTB case and after 60km fiber transmission.

edges. For the case of $W_G = 2$ GHz, in the first branch, an OBPF with 17 GHz bandwidth and upper edge at 193.1075THz is used to suppress the OC at 193.109THz; in the second and third branches, the same OBPFs with 15 GHz bandwidth and central frequency of 193.1 GHz are used to suppress the two OCs simultaneously; in the fourth branch, an OBPF with 17 GHz bandwidth and lower edge at 193.0925THz is used to suppress the OC at 193.091 THz. Their optical spectra after filtering are shown in Fig. 2 (g)-(j). Next, the first two beams are injected into the first BPD pair, including PD1 and PD2, and are converted to electrical signal, and the latter two are injected into the second BPD pair, including PD3 and PD4. The four PDs have same responsivity of 1mA/mW and thermal noise power density of 10^{-24} W/Hz. The RF spectra of four photocurrents are shown in Fig. 2 (k)$\sim$(n). It can be seen that the photocurrents from PD1 and PD4 consist of the desired RF OFDM signals and SSBIs with partially overlapped spectra, while these from PD2 and PD3 consist only of the SSBIs. The differentiate photocurrents output from the two BPDs consist mainly of the RF OFDM signals, as shown by the RF spectra in Fig. 2 (p) and (q), which means that the SSBIs are cancelled out after differentiate circuits although some residual SSBIs exist at low frequency, which attributes to the non-ideal filter edges. Then, the RF OFDM signals are IQ demodulated to the baseband ones. The baseband OFDM signals are digital signal processed, which is performed in a reverse process to the DSP at transmitter. The constellations of the demodulated 16-QAM signals at optical back-to-back (OBTB) case are given in Fig. 2 (s) and (t), which show that two OFDM signals are received correctly. Finally, the link performance is estimated according to the calculated EVM with Matlab module.

To check the influence of the GB on the PDM SSB-OOFDM link, the EVMs of the received signals at different GB for two channels at OBTB case and after 60-km fiber transmission are calculated based on the simulation, as given in Fig. 3. It can be seen that the EVMs keep constant at about 7% and 10% as the GB is larger than 2 GHz for the two cases, although the EVMs go beyond 16.3% for the cases of GB $=$ 1 GHz and 0.5 GHz. This means that the link does not suffer from SSBIs, but is degraded by the nonideal edges of the OBPFs, especially as the GB is small (W_G $<$2 GHz). In fact, smaller GB of the SSB-OOFDM signals needs sharper OBPF edges, which throws down a serious challenge to the system, so it requires a trade-off between the SE and the implement complexity. The implement complexity of filtering can be loosened by reasonably increasing the GB.

To emphasis the robust of our proposed BICR in terms of insensitivity to the PMD and immunity to the SSBI, another three cases of SSB-OOFDM systems are simulated for comparison additionally. In the first case, the single polarization 56Gbps 16-QAM SSB-OOFDM is transmitted and directly detected by a single PD. The curves of the EVM versus the GB at OBTB case and after 60-km fiber transmission are shown in Fig. 4(a). It can be seen that the EVM increases rapidly as the GB reduces due to the SSBI while the EVM approaches to that of our proposed scheme as

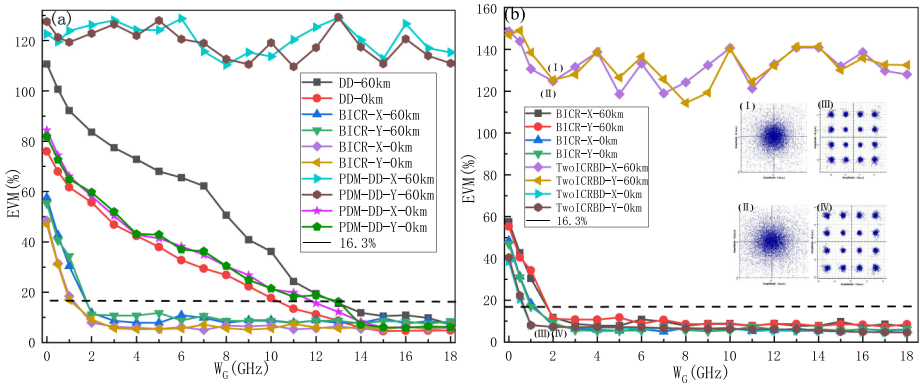

Fig. 4. (a) The EVMs versus GB for the PDM IM/DD SSB-OOFDM, IM/DD SSB-OOFDM and our proposed BICR-based PDM SSB-OOFDM system and (b) the EVMs of PDM SSB-OOFDM system with two ICRBDs and our proposed PDM SSB-OOFDM system with BICR at the OBTB and after 60 km fiber transmission.

W_G>14 GHz since the SSBI is almost nonoverlapped with RF-OOFDM signal in the frequency domain. This means that our scheme can cancel the SSBI perfectly even if the guard band is reduced to 2 GHz. The second case has the same transmitter and transmission link as our proposed scheme but the PDM SSB-OOFDM signal is split by a PBS for polarization demultiplexing and two PDs for direct detection in a traditional way. The curves of the EVM versus the GB for the two polarizations at the OBTB case and after 60-km fiber transmission are also shown in Fig. 4(a). The curves of the EVM versus the GB at the OBTB case are similar to the first case. This means that the PDM SSB-OOFDM signal can be polarization demultiplexed by the PBS correctly to two orthogonal SSB-OOFDM signals since they do not couple with each other before fiber transmission, while both SSB-OOFDM signals suffer from only the SSBI. However, after 60km fiber transmission, the EVMs of the two SSB-OOFDM signals increase to about 120% for all GBs. This means that the two orthogonal SSB-OOFDM signals are coupled with each other by random polarization rotation due to the fiber PMD and cannot be directly decoupled by the PBS. For the third case, the PDM SSB-OOFDM system has the same transceiver equipment as in [26] but without MIMO algorithm. As shown in Fig. 4(b), the EVM of the PDM SSB-OOFDM system with two ICRBDs has been fluctuating above 100% after fiber transmission, which means that the system cannot also demultiplex the received PDM SSB-OOFDM signal due to the PMD. However, the EVM of our proposed PDM SSB-OOFDM system with the BICR keeps at around 10% when the GB is greater than 2 GHz, which means that our proposed PDM SSB-OOFDM system can overcome the PMD interference and demultiplex two SSB-OOFDM signals correctly. The constellations of the demodulated two OFDM signals at X- and Y-polarization directions from the received PDM SSB-OOFDM signals with a GB of 2 GHz are shown in Fig. 4(b). It can be seen that the data cannot be recovered by two ICRBDs since the two SSB-OOFDM signals cannot be decoupled by PBS, as shown by the constellation diagrams (I) and (II) in Fig. 4(b) for the two polarization directions, while our proposed scheme can recover the data correctly, as shown by the constellation diagrams (III) and (IV) in Fig. 4(b).

To further check the transmission performance with our proposed BICR, we measure the EVMs of the received PDM SSB-OOFDM signal at $W_G = 2$ GHz and CSPR = 12dB, after different lengths of SSMF transmission, as given in Fig. 5. It can be seen that the EVMs on the two polarization directions increase almost synchronously as the fiber transmission distance extends, while the EVMs keep below the FEC of 16.3% with a difference smaller 1% on the two polarization even if the fiber transmission distance increases to 120km. Fig. 5(I)-(IV) are the constellation diagrams of the optical signal at the X- and Y-polarization directions after 60 and 120 km fiber transmission.

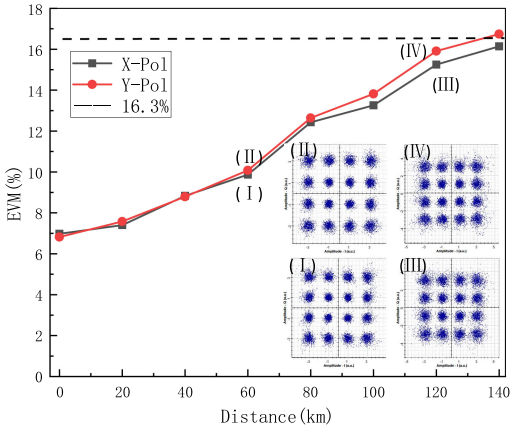

Fig. 5. EVM versus the fiber transmission distance when CSPR = 12dB and GB = 2 GHz.

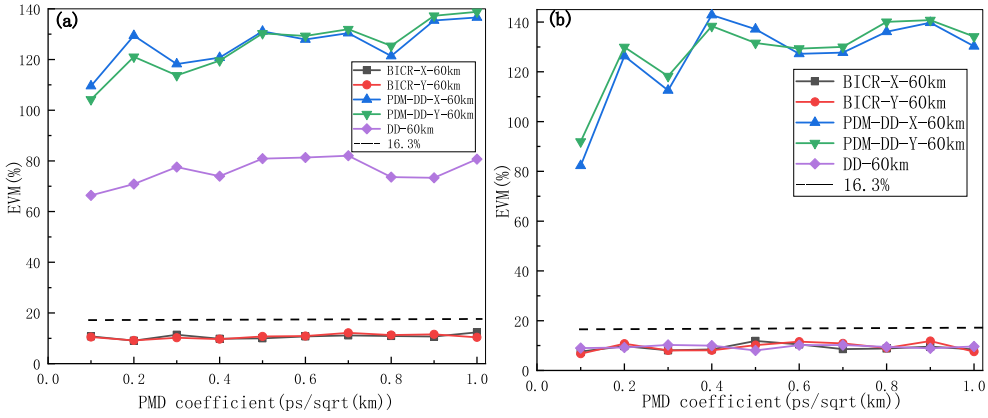

Fig. 6. After 60 km fiber transmission, the EVM of PDM IM/DD SSB-OOFDM, IM/DD SSB-OOFDM and PDM SSB-OOFDM with BICR versus PMD coefficient (a) GB is set to 4 GHz. (b) GB is set to 14 GHz.

To examine the influence of the PMD on our proposed scheme, the PMD coefficient is swept from 0.1 to 1.0 ps/km$^{1/2}$ for three cases: the PDM SSB-OOFDM system, single-polarization IM/DD SSB-OOFDM system and PDM IM/DD SSB-OOFDM system after 60km fiber transmission with W_G = 4 GHz and W_G = 14 GHz. The curves of the EVMs versus PMD are shown in Fig. 6(a) and (b). As shown in Fig. 6 (a), the EVM of the PDM IM/DD SSB-OOFDM system has always been higher than 100% for the PMD and the EVM of the single-polarization IM/DD SSB-OOFDM system has remained above 60% for the SSBI is partly overlapped with the demodulated RF-OFDM signal in the photocurrent in frequency domain. Only the EVM of our proposed PDM SSB-OOFDM system with BICR maintains about 10%. When GB is set to 14 GHz, the SSBI distortion is avoided for all cases and Fig. 6(b) shows that the EVMs of the single-polarization IM/DD SSB-OOFDM system and our proposed BICR scheme remain about 10% and almost constant as the PMD varies from 0.1 to 1.0 ps/km$^{1/2}$, while the EVM of the PDM IM/DD SSB-OOFDM system still keeps about 120%. This is because the fiber PMD rotates the polarization state of the PDM SSB-OOFDM signal randomly and makes the two SSB-OOFDM signals couple with each other. Our proposed BICR can decouple the PDM SSB-OOFDM signal and has the same immunity to the PMD as the single-polarization IM/DD SSB-OOFDM system. Compared with the other two cases, the PDM

SSB-OOFDM system with our proposed BICR can not only cancel the SSBI, but also is immune to the fiber PMD.

4. Conclusion

In this paper, we demonstrate a novel BICR for PDM SSB-OOFDM systems, which has an improved SE by polarization multiplexing and a reduced GB via SSBI cancellation. Since the BICR is implemented by polarization-insensitive optical power split and OBPFs without polarization stabilizer and polarization beam splitter, the receiver is insensitive to the fiber PMD. A simulation link with 112Gbps 16-QAM PDM SSB-OOFDM signals is built to demonstrate our proposed BICR. The EVMs of the received two SSB-OOFDM signals keep below the FEC limit of 16.3% even after 120km fiber transmission. The simulation results agree well with our theoretical analysis.

References

[1] J. S. Wey and J. Zhang, "Passive optical networks for 5G transport: Technology and standards," *J. Lightw. Technol.*, vol. 37, no. 12, pp. 2830–2837, 2018.

[2] W. Jin, C. Zhang, C. Chen, Q. Zhang, and K. Qiu, "Scalable and reconfigurable all-optical VPN for OFDM-based metro-access integrated network," *J. Lightw. Technol.*, vol. 32, no. 2, pp. 318–325, 2013.

[3] Z. Cao, J. Yu, W. Wang, L. Chen, and Z. Dong, "Direct-detection optical OFDM transmission system without frequency guard band," *IEEE Photon. Technol. Lett.*, vol. 22, no. 11, pp. 736–738, Jun. 2010.

[4] C. Zhang, J. Huang, C. Chen, and K. Qiu, "All-optical virtual private network and ONUs communication in optical OFDM-based PON system," *Opt. Exp.*, vol. 19, no. 24, pp. 24816–24821, 2011.

[5] W. Bao, M. Bi, S. Xiao, J. Fang, T. Huang, and Y. Zhang, "Lagrange interpolation based extended kalman filter for phase noise suppression in CO-OFDM system," *Opt. Commun.*, vol. 435, pp. 221–226, 2019.

[6] J. Ma, "Influence of the device parameters in ICRBD on SSB-OOFDM signal with reduced guard band," *Opt. Exp.*, vol. 22, no. 24, pp. 29636–29654, 2014.

[7] J. Ma, "Simple signal-to-signal beat interference cancellation receiver based on balanced detection for a single-sideband optical OFDM signal with a reduced guard band," *Opt. Lett.*, vol. 38, no. 21, pp. 4335–4338, 2013.

[8] W. R. Peng, I. Morita, and H. Tanaka, "Enabling high capacity direct-detection optical OFDM transmissions using beat interference cancellation receiver," in *Proc. 36th Eur. Conf. Exhib. Opt. Commun.*, 2010, Paper Tu.4.A.2.

[9] Y. Qiu, M. Luo, Z. He, and X. Li, "Balanced detection of 100-Gb/s optical OFDM signals with SSBI cancellation based on fused-type fiber mode-selective coupler," *IEEE Photon. J.*, vol. 10, no. 5, Oct. 2018, Art. no. 7105010.

[10] Y. Zhang and J. Ma, "Colorless beat interference cancellation receiver for the orthogonally polarized SSB-OOFDM signal with reduced guard band," *Appl. Opt.*, vol. 55, no. 26, pp. 7371–7377, 2016.

[11] Y. Zhang and J. Ma, "A new beat interference cancellation receiver with 3×3 optical coupler for the SSB-OOFDM signal with reduced guard band," *Opt. Commun.*, vol. 367, pp. 279–285, 2016.

[12] W. R. Peng *et al.*, "Spectrally efficient direct-detected OFDM transmission employing an iterative estimation and cancellation technique," *Opt. Exp.*, vol. 17, no. 11, pp. 9099–9111, 2009.

[13] W. R. Peng, B. Zhang, K. M. Feng, X. Wu, A. E. Willner, and S. Chi, "Spectrally efficient direct-detected OFDM transmission incorporating a tunable frequency gap and an iterative detection techniques," *J. Lightw. Technol.*, no. 27, no. 24, pp. 5723–5735, 2009.

[14] A. Mecozzi, C. Antonelli, and M. Shtaif, "Kramers–Kronig coherent receiver," *Optica*, vol. 3, no. 11, pp. 1220–1227, 2016.

[15] Z. Li *et al.*, "SSBI mitigation and the Kramers–Kronig scheme in single-sideband direct-detection transmission with receiver-based electronic dispersion compensation," *J. Lightw. Technol.*, vol. 35, no. 10, pp. 1887–1893, 2017.

[16] C. C. Wei, C. T. Lin, and C. Y. Wang, "PMD tolerant direct-detection polarization division multiplexed OFDM systems with MIMO processing," *Opt. Exp.*, vol. 20, no. 7, pp. 7316–7322, 2012.

[17] C. Li *et al.*, "100.29-Gb/s direct detection optical OFDM/OQAM 32-QAM signal over 880 km SSMF transmission using a single photodiode," *Opt. Lett.*, vol. 40, no. 7, pp. 1185–1188, 2015.

[18] P. Yang, J. Ma, and J. Zhang, "A polarization-division multiplexing SSB-OFDM system with beat interference cancellation receivers," *Opt. Commun.*, vol. 416, pp. 137–144, 2018.

[19] Y. Zhu, M. Jiang, and F. Zhang, "Direct detection of polarization multiplexed single sideband signals with orthogonal offset carriers," *Opt. Exp.*, vol. 26, no. 12, pp. 15887–15898, 2018.

[20] Z. Hu and J. Ma, "Misaligned optic carrier polarization division multiplexing SSB-OOFDM system based on a beat interference cancellation receiver," *OSA Continuum*, vol. 2, no. 10, pp. 2935–2947, 2019.

[21] X. Li *et al.*, "Asymmetric direct detection of orthogonal offset carriers assisted polarization multiplexed single-sideband signals," *Opt. Exp.*, vol. 28, no. 3, pp. 3226–3236, 2020.

[22] C. Sun, D. Che, H. Ji, and W. Shieh, "Investigation of single-and multi-carrier modulation formats for Kramers–Kronig and SSBI iterative cancellation receivers," *Opt. Lett.*, vol. 44, no. 7, pp. 1785–1788, 2019.